

FILE COPY
No. /

**Not to Be removed
from Library**

FILE COPY
To be returned to the Files of
Ames Aeronautical Laboratory
National Advisory Committee
for Aeronautics
Moffett Field, Calif.

TN 641

~~11055~~
~~109~~

TECHNICAL NOTES
NATIONAL ADVISORY COMMITTEE FOR AERONAUTICS

No. 641

INTERFERENCE OF WING AND FUSELAGE FROM TESTS OF
17 COMBINATIONS IN THE N.A.C.A. VARIABLE-DENSITY TUNNEL
COMBINATIONS WITH SPECIAL JUNCTURES

By Albert Sherman
Langley Memorial Aeronautical Laboratory

Washington
March 1938

NATIONAL ADVISORY COMMITTEE FOR AERONAUTICS

TECHNICAL NOTE NO. 641

INTERFERENCE OF WING AND FUSELAGE FROM TESTS OF
17 COMBINATIONS IN THE N.A.C.A. VARIABLE-DENSITY TUNNEL
COMBINATIONS WITH SPECIAL JUNCTURES

By Albert Sherman

SUMMARY

As part of the wing-fuselage interference program in progress in the N.A.C.A. variable-density wind tunnel, a method of eliminating the interference burble associated with critical midwing combinations was investigated. The interference burble of the critical midwing combination was shown to respond to modifications at the nose of the juncture and to be entirely suppressed with little or no adverse effect on the high-speed drag by special leading-edge fillets.

INTRODUCTION

An extensive program of research is being conducted in the N.A.C.A. variable-density wind tunnel on the interference between wing and fuselage at large values of the Reynolds Number (references 1, 2, 3, and 4). Reference 1 outlined the wing-fuselage interference program and presented the initial and basic parts thereof, comprising test results for 209 combinations that represented, to the widest practical extent, the most important parameters of combination, such as: wing position relative to the fuselage, wing shape, juncture shape, and fuselage shape. The discussion therein was fundamental in nature and treated the interpretation of wing-fuselage interference.

It was soon evident that many combinations having excellent high-speed drag characteristics would be barred from consideration in any practical design problem because of low maximum lifts. Specifically, the unfavorable ones were mainly midwing combinations of round fuselages and low-drag efficient airfoils of moderate thickness and small camber (e.g., the N.A.C.A. 0012). A premature flow break-

down, or interference burble, was usually associated with such midwing combinations, whether or not split flaps were employed (reference 4), and was responsible for the low maximum lifts. Interference burbles may vary in character and severity, however, and may not seriously reduce the maximum lift, as was demonstrated by some unfilleted low-wing combinations. The different types of interference burble were discussed in reference 1.

In the investigation reported herein, a study of the interference burble of the critical midwing combination was made and a means for its elimination was derived. The descriptions in table V of the combinations tested indicate the scope of the experimental investigation.

MODELS AND TESTS

The wing models employed were rectangular 5- by 30-inch duralumin airfoils of N.A.C.A. 0012, N.A.C.A. 4412 (see reference 1), and N.A.C.A. 23012 (reference 5) profiles. The N.A.C.A. 0012 and 4412 airfoils are "standard" for the wing-fuselage interference investigation. The N.A.C.A. 23012 was included to show the effect on the interference associated with the use of a more recent profile. These wings were combined only with the round fuselage (reference 1), which is an airship form of polished duralumin, 20.156 inches in length, having a fineness ratio of 5.86. The split flaps were made of brass plate and had sharpened trailing edges. They were 20 percent of the wing chord in width, were full-span, and had the deflections indicated in table V. The junctures and fillets were formed of plaster of paris with either of two finishes: smoothly finished plaster, or carefully rubbed and polished lacquer. The type of finish for each combination is specified in the third column of table V. Following the tests reported herein, the lacquered finish was adopted as standard. Photographs of representative combinations are shown in figures 1 to 4.

The tests were performed in the variable-density wind tunnel (reference 6) at a test Reynolds Number of approximately 3,100,000 (effective $R = 8,200,000$). In addition, values of the maximum lift coefficient were obtained at a reduced speed corresponding to a test Reynolds Number of approximately 1,400,000 (effective $R = 3,700,000$). The testing procedure and test precision, which are practically

the same as for an airfoil alone, are fully described in reference 1. Since the tests of reference 1 were made, a small additional correction of less than -1 percent has been applied to the measurement of the dynamic pressure q to improve the precision of the results.

RESULTS

The test data are given in the same manner as in reference 1, in which the methods of analysis and of presentation of the results are fully discussed.

As in the preceding reports of the interference program (references 1, 2, 3, and 4), the test results are given in tables supplemented by figures. Table I contains the characteristics of the wings alone and table II, those of the fuselage. Table III presents the sums of the fuselage characteristics and the interferences at various angles of attack for each of the combinations tested. The values given represent the differences between the characteristics of each combination and those of the wing alone or of the wing with a full-span split flap. Obviously, the characteristics of the combinations themselves can, if desired, be obtained by adding corresponding items in tables I and III. Table IV of the program (see reference 1), which presents interference data for disconnected combinations, is not continued herein because no additional combinations of this character were investigated.

Table V contains the combination diagrams and descriptions in addition to the principal aerodynamic characteristics of the combinations. The values d/c and k/c represent the longitudinal and vertical displacements, respectively, of the wing quarter-chord axis measured (in chord lengths) positive ahead of and above the quarter-length point of the fuselage axis; i_w is the angle of wing setting.

The last nine columns of the table present the following important characteristics as standard nondimensional coefficients based on the original wing areas of 150 square inches:

- a, lift-curve slope (in degree measure) as determined in the low-coefficient range for an effective aspect ratio of 6.86. This value of

the aspect ratio differs from the actual value for the models because the lift results are not otherwise corrected for tunnel-wall interference. For the combinations with split flaps, values averaged over the useful range of lift coefficient are given.

- e, Oswald's airplane, or span, efficiency factor.
(See reference 1.)
- $C_{D_{e_{min}}}$, minimum effective profile-drag coefficient
 $\left(C_D - \frac{C_L^2}{\pi A} \right)_{min}$. For the combinations with split flaps, average values of the drag taken over the useful range of lift coefficient and accurate to within about 5 percent are given instead.
- $C_{L_{opt}}$, optimum lift coefficient, i.e., the lift coefficient corresponding to $C_{D_{e_{min}}}$.
- n_o , aerodynamic-center position indicating approximately the location of the aerodynamic center ahead of the wing quarter-chord axis as a fraction of the wing chord. Numerically, n_o equals $\frac{dC_{m_{c/4}}}{dC_L}$ at zero lift.
- C_{m_o} , pitching-moment coefficient at zero lift about the wing quarter-chord axis. For the combinations with split flaps, average values of the moment taken over the useful range of lift coefficient and accurate to within about 5 percent are given instead.
- $C_{L_{lib}}$, lift coefficient at the interference burble, i.e., the value of the lift coefficient beyond which the air flow has a tendency to break down as indicated by an abnormal increase in the drag.
- $C_{L_{max}}$, maximum lift coefficient given for two different values of the effective Reynolds Number. (See reference 1.) The turbulence factor om-

ployed in this report to obtain the effective R from the test R is 2.64.

As in reference 2, the values of the effective Reynolds Number differ somewhat from those given in reference 1 because of a later more accurate determination of the turbulence factor for the tunnel. The values of the effective Reynolds Number given in reference 1 are subject to correction by a factor of 1.1.

Figures 5 to 7 present the variation with angle of attack of the aerodynamic characteristics for certain combinations, grouped so as to illustrate the effects of variations in the interesting parameters of combination. Angle-of-attack plots are more effective than polars for showing the character of the lift-curve peaks.

DISCUSSION

Mechanism of the interference burble.- The phenomenon of the interference burble (i.e., a premature flow breakdown induced by the presence of an interfering body) associated with many wing-fuselage combinations was discussed in reference 1. That discussion will now be analyzed with the purpose of clarifying the picture of the interference burble and of describing the measures effected for its suppression.

The origin of such a flow breakdown may be ascribed to the action of two types of interference: boundary-layer interference and potential-flow interference. The term "boundary-layer interference" refers to the changes produced in the boundary layer of one body by the presence of another body. Similarly, potential-flow interference refers to the changes produced in the potential field associated with one body by the presence of another body. As the interference burble is a separation phenomenon, it is desirable that the interferences should be considered on the basis of their operation toward developing separation.

Consider the simple case of the rectangular N.A.C.A. 0012 airfoil intersecting a large thin flat plate disposed in its X-Z plane of symmetry. At a moderately high angle of attack, the boundary layer of the plate must be drawn

into the low-pressure area extending over the upper surface of the contiguous airfoil sections. The inducted low-energy air obviously thickens the boundary layer of the airfoil and reduces its resistance to the onset of separation. This boundary-layer interference, then, causes a premature stall of the juncture sections as the angle of attack is increased.

Now, if the plain flat plate is replaced by an air-ship-shape fuselage in a conventional arrangement, potential-flow interferences are introduced. If the trace of the fuselage in a Y-Z plane immediately ahead of the root-section leading edge is considered, it can be seen that the induced upflow associated with the lift must have components of flow in this plane that produce a flow pattern about the fuselage trace analogous to the potential-flow pattern about a cylinder. A short distance back of the airfoil leading edge, this flow pattern tends to disappear. From the analogy of the potential flow about a cylinder, such a flow can be considered as producing positive pressure increments at the nose of the wing roots for the high-wing and low-wing combinations. For the midwing combination, however, it would produce negative pressure increments. These positive and negative pressure increments are equivalent, respectively, to favorable and adverse pressure-gradient components in the stream direction at the wing roots.

At the rear of the upper surface of the wing roots, the geometry of the combination describes a region of divergence in the low-wing condition and of convergence in the high-wing condition, as compared with the wing alone. At the nose of the juncture, these conditions are reversed. Divergences and convergences induce, respectively, adverse and favorable pressure gradients,

Consider now a high-wing combination of the round fuselage and the rectangular N.A.C.A. 0012 airfoil at an angle of attack corresponding to a moderately high lift coefficient. A low-pressure peak exists at the nose of the airfoil section and is followed by rising pressures in the direction of the trailing edge; in other words, there is an adverse pressure gradient. As the angle of attack is increased, the boundary-layer flow finally fails to progress against the growing pressure gradient and separation ensues. For the N.A.C.A. 0012 section the drop in lift is large, the separation is sudden, and it is critically affected by conditions near the leading

edge. (See discussion in reference 7 relative to stalling.) At the juncture, however, this picture of the stalling process is modified. Both boundary-layer and potential-flow interferences are operating. The boundary-layer interference and the divergence at the nose are both promoting early separation. The convergence at the rear of the juncture and the Y-Z plane component of flow, previously mentioned, are influences toward reducing the adverse pressure gradients over the upper surface of the juncture sections and thus delaying the burble. On the other hand, the tendency of the downwash distribution to maintain the load distribution over the wing-fuselage juncture may act to overload the root sections and cause an earlier stall. The combined effects of the interferences, however, are apparently small for the high-wing combination; the interference burble does not occur appreciably before the maximum lift, which is about the same as for the wing alone. (See table V, reference 1.) The substitution of different wing profiles does not change this result.

The corresponding low-wing combination is subject to the same types of interference as just described, except that the regions of divergence and convergence are interchanged at the wing root. At a moderate angle of attack the various interferences produce separation over the upper surface of the wing at the rear portion of the juncture (the interference burble). As the lift is increased with angle of attack, the dead air drifts outward, progressively increasing the area covered by separated flow and making it more difficult for the flow to maintain itself over the leading edge than in the unseparated condition at the same lift coefficient. The potential-flow interference at the nose of the wing root apparently acts to inhibit early flow breakaway there, and the combination continues to develop lift, but at a lower rate than before the occurrence of the interference burble, until the angle of maximum lift is reached. A more or less sudden separation of the flow over most of the upper surface then occurs. The value of maximum lift, however, does not appear to be seriously reduced by the early trailing-edge separation of the root sections. (See reference 1.) It should therefore be evident how an expanding fillet that fills the divergence at the rear of the juncture alleviates this form of interference burble and how the substitution of different airfoil sections (which can produce little change in the expansion of the juncture) can have only a

small effect on the occurrence of the burble. (Compare reference 1.)

The midwing combination presents a somewhat different picture. The component of flow in the Y-Z plane now acts to increase the adverse pressure gradient over the forward portions of the contiguous airfoil sections. The interference of the fuselage on the load grading overloads those same sections, and the boundary-layer interference also operates to induce a premature burble. The result is an early interference burble when the airfoil is, like the N.A.C.A. 0012, sensitive to leading-edge stalling. In other words, the interferences combine to produce a separation of flow from the leading edge of the root sections at a moderate angle of attack. As the angle of attack is increased, the combination continues to gain lift, but more slowly. The value of maximum lift is low, however, since the entire center portion has been stalled well before the angle of maximum lift is reached.

Suppression of the midwing interference burble.- In the investigation reported in reference 1, plan-form fillets designed to unload the wing-root sections were added to the critical midwing combination of the round fuselage and rectangular N.A.C.A. 0012 airfoil. Very little effect was produced as regards the interference burble or the value of maximum lift. The same result had previously been found for ordinary tapered fillets.

Marked effect in delaying the interference burble and minimizing the loss in maximum lift coefficient resulted when the wing-root sections were changed to less sensitive profiles, that is, profiles showing moderate adverse pressure gradients in the leading-edge regions (e.g., the rectangular N.A.C.A. 4412 and the tapered N.A.C.A. 0018-09 airfoils (reference 1)). Since cambered or thick airfoils, however, exhibit too large values of high-speed drag coefficient, it is desirable to suppress the interference burble associated with low-drag airfoils of the critical type in midwing combinations.

Surface finish at the juncture.- Surface finish is known to have a powerful effect upon boundary-layer phenomena. At very low Reynolds Numbers, a roughened airfoil surface may show a tendency to increase the maximum lift coefficient through inducing earlier transition. (See the discussion in reference 7 relative to scale effect

on maximum lift.) At the usual flight values of Reynolds Number, however, transition generally occurs so close to the separation point at high angles of attack that the effect of surface roughness is mainly to increase the thickness of the boundary layer. Thickened boundary layers are less resistant to separation than thin ones.

In the investigation of combinations with split flaps (reference 4), a combination of the round fuselage and rectangular N.A.C.A. 23012 airfoil in a semihigh-wing position was included to determine the interference associated with this modern section in an efficient combination. An adverse interference on maximum lift was evident. In the investigation reported herein, the elimination of this effect was first attempted. The tapered fillet for the combination with split flaps was modified to effect a change in the wing-root sections. The forward portion of the fillet was enlarged, extended, and drooped to simulate noncritical airfoil profiles (combination 289; leading-edge fillet 1 as in figure 1). A further adverse effect on the maximum lift coefficient resulted. The wing-fuselage models heretofore were formed with plaster of paris junctures or with fillets having carefully smoothed surfaces. It was doubted, however, that these surfaces were sufficiently smooth to minimize boundary-layer interference due to surface roughness. A carefully rubbed and polished lacquered finish, therefore, was next applied to the plaster surfaces at the juncture and the combination retested. The result was a definite improvement in the maximum lift. (Compare combinations 289 and 290, table V.) At this point, it was decided to continue the investigation (as regards suppressing the interference burble) in a systematic manner with the midwing combination of the round fuselage and the rectangular N.A.C.A. 0012 airfoil, which is the standard critical combination in the wing-fuselage interference program.

The new polished lacquer finish was applied to the plaster surfaces at the juncture of this midwing combination but showed no appreciable effect on the onset of the interference burble or the low maximum lift. When the new finish was applied to the same combination with ordinary tapered fillets, however, an appreciable increase resulted in the maximum lift of the same order of magnitude as that shown by combination 290, and the interference burble was delayed (fig. 5). The gain, however, did not eliminate the adverse interference of the fuselage. It appears that a high degree of refinement in surface

finish is relatively ineffective on combinations showing strong unfavorable potential-flow interferences and, conversely, (it may be inferred) that a good combination might be improved by a very smooth surface finish, especially in critical regions.

Leading-edge fillets.- The parameter of combination that had most effect upon the interference of the midwing condition was the wing profile. Moderate-camber or thick wing sections showed little susceptibility to an interference burble. The explanation is, probably, that the non-critical flow conditions at the leading edge associated with such profiles (as contrasted with the N.A.C.A. 0012, for example) are capable of absorbing the interference of the fuselage without serious results.

The next step was, therefore, to change systematically the root sections of the critical midwing combinations to less sensitive profiles by means of fillets. A series of such fillets was investigated (leading-edge fillets 2, 2a, 2b; combinations 294, 295, 296, 297) that extended 0.45c laterally from the wing root and various distances forward from the leading edge. (See figs. 2 and 3.) The forward portions of the fillets were drooped, had increased leading-edge radii, and were faired into the wing and fuselage. They were all successful in that they raised the value of the maximum lift of the combination to the neighborhood of that of the wing alone, suppressed the interference burble, and increased the minimum drag only slightly. Their characteristics improved as the amount of the forward projection of the fillet beyond the usual wing leading edge was reduced. A second series was therefore investigated (leading-edge fillets 3, 3a, 3b, 3c, 3d; combinations 298, 299, 300, 302, 303, 304) in which the nose length of the fillet was practically zero and the span length was varied. At the intersection the fillet was made to form the N.A.C.A. 43018 (3.8-percent camber at 15 percent behind the leading edge) section (reference 8) with its zero lift direction agreeing with that of the wing. (See fig. 4.)

Fillets with span lengths 0.15c, or greater, raised the value of the maximum lift to equal or exceed that of the wing alone; the longer the span length, the higher the maximum lift (fig. 6). Little gain, however, was obtainable by lengths greater than 0.3c. Other effects of the series 3 of leading-edge fillets were: The suppression

of the interference burble before the stall and the absence of adverse influence on the minimum drag; and the enabling of split flaps, when applied to the critical midwing combinations, to realize their full increment. (See table V.) It is interesting to note that the maximum lift obtained with split flaps and leading-edge fillets applied to the midwing combination of the N.A.C.A. 0012 airfoil (combination 300) was practically the same as that obtained when a medium-cambered airfoil (N.A.C.A. 4412) with ordinary tapered fillets (combination 301) was substituted. The minimum drag and pitching moments for the N.A.C.A. 4412 airfoil combination, flaps retracted, however, were very much greater than for the N.A.C.A. 0012 airfoil combination. (See reference 1.)

The relative influence of the leading-edge and trailing-edge portions of a fillet is indicated in figure 7, which presents the characteristics for midwing combinations with various fillets. When the tapered fillet is considered, however, the effects of the radius at the leading edge should be borne in mind; and, when the leading-edge fillet alone with the trailing-edge portion removed is considered, the adverse effect on the divergence should be noted. Nevertheless, the figure demonstrates plainly that a fillet designed to counteract the interference at both ends of the wing-root chord is the most effective. Such behavior is in accordance with the nature of leading-edge and trailing-edge stalling as discussed in reference 7.

Application of Leading-Edge Fillets

In figures 5 to 7 many double lift-curve peaks are noticeable. Where the double peaks are both sharp, the lift at the first peak fairly high, and the drops nearly equal, the explanation is probably that one wing panel is stalling ahead of the other. The lift curve in figure 7 for combination 292 illustrates how double peaks might appear when the wing center stalls early, the tips following gradually. The center stall is a highly desirable characteristic for an airplane from considerations of control and stability. For this reason, the use of leading-edge fillets might sometimes be inadvisable. They can be employed to advantage, however, to fillet outboard nacelles on multiengine airplanes. Leading-edge fillets, where used, should be provided with very smooth surfaces for most effective results.

Langley Memorial Aeronautical Laboratory,
National Advisory Committee for Aeronautics,
Langley Field, Va., February 9, 1938.

REFERENCES

1. Jacobs, Eastman N., and Ward, Kenneth E.: Interference of Wing and Fuselage from Tests of 209 Combinations in the N.A.C.A. Variable-Density Tunnel. T.R. No. 540, N.A.C.A., 1935.
2. Sherman, Albert: Interference of Wing and Fuselage from Tests of 28 Combinations in the N.A.C.A. Variable-Density Tunnel. T.R. No. 575, N.A.C.A., 1936.
3. Sherman, Albert: Interference of Wing and Fuselage from Tests of 30 Combinations in the N.A.C.A. Variable-Density Tunnel. Combinations with Triangular and Elliptical Fuselages. T.R. No. (to be published), N.A.C.A., 1938.
4. Sherman, Albert: Interference of Wing and Fuselage from Tests of 18 Combinations in the N.A.C.A. Variable-Density Tunnel. Combinations with Split Flaps. T.N. No. 640, N.A.C.A., 1938.
5. Jacobs, Eastman N., and Clay, William C.: Characteristics of the N.A.C.A. 23012 Airfoil from Tests in the Full-Scale and Variable-Density Tunnels. T.R. No. 530, N.A.C.A., 1935.
6. Jacobs, Eastman N., and Abbott, Ira H.: The N.A.C.A. Variable-Density Wind Tunnel. T.R. No. 416, N.A.C.A., 1932.
7. Jacobs, Eastman N., and Sherman, Albert: Airfoil Section Characteristics as Affected by Variations of the Reynolds Number. T.R. No. 586, N.A.C.A., 1937.
8. Jacobs, Eastman N., Pinkerton, Robert M., and Greenberg, Harry: Tests of Related Forward-Camber Airfoils in the Variable-Density Wind Tunnel. T.R. No. 610, N.A.C.A., 1937.

TABLE I - AIRFOIL CHARACTERISTICS

Airfoil	C_L	C_{De}	$C_{mC/4}$	C_L	C_{De}	$C_{mC/4}$	C_L	C_{De}	$C_{mC/4}$
	$\alpha = 0^\circ$			$\alpha = 4^\circ$			$\alpha = 12^\circ$		
Rectangular N.A.C.A. 0012	0.000	0.0080	0.000	0.307	0.0087	0.003	0.920	0.0150	0.004
Rectangular N.A.C.A. 23012	.090	.0085	-.006	.400	.0095	-.004	1.025	.0161	-.007
Rectangular N.A.C.A. 0012 with 0.2c split flap deflected 60°	.975	.1718	-.204	1.268	.1736	-.207	1.819	.1755	-.213
Rectangular N.A.C.A. 23012 with 0.2c split flap deflected 60°	1.049	.1726	-.207	1.341	.1738	-.211	1.895	.1754	-.218
	$\alpha = -4^\circ$			$\alpha = 0^\circ$			$\alpha = 8^\circ$		
Rectangular N.A.C.A. 4412	-0.006	0.0097	-.809	0.298	0.0095	-.087	0.899	0.0136	-.084

TABLE II - FUSELAGE CHARACTERISTICS

Fusel- lage	En- gine	C_L	C_D	${}^1C_{mF}$	C_L	C_D	${}^1C_{mF}$	C_L	C_D	${}^1C_{mF}$	C_L	C_D	${}^1C_{mF}$	C_L	C_D	${}^1C_{mF}$
		$\alpha = 0^\circ$			$\alpha = 4^\circ$			$\alpha = 8^\circ$			$\alpha = 12^\circ$			$\alpha = 16^\circ$		
Round	None	0.000	.0041	.000	.001	.0042	.016	.005	.0049	.028	.011	.0062	.035	.019	.0085	.038

¹Pitching-moment coefficient about the quarter-chord point of the fuselage.

TABLE III - LIFT AND INTERFERENCE, DRAG AND INTERFERENCE, AND PITCHING MOMENT
 AND INTERFERENCE OF FUSELAGE IN WING-FUSELAGE COMBINATIONS

Combi- nation	ΔC_L	ΔC_{D_e}	$\Delta C_{m_{c/4}}$	ΔC_L	ΔC_{D_e}	$\Delta C_{m_{c/4}}$	ΔC_L	ΔC_{D_e}	$\Delta C_{m_{c/4}}$
	$\alpha = 0^\circ$			$\alpha = 4^\circ$			$\alpha = 12^\circ$		
¹ 289	-0.076	-0.0108	0.012	-0.056	-0.0101	0.016	-0.027	-0.0068	0.030
¹ 290	-	-	-	-	-	-	-	-	-
¹ 291	-	-	-	-	-	-	-	-	-
292	.003	.0035	-.002	.026	.0040	.005	.058	.0055	.016
293	.003	.0034	-.002	.035	.0036	.003	.071	.0050	.012
294	.012	.0038	-.003	.037	.0041	.010	.090	.0044	.034
295	.003	.0042	-.002	.030	.0042	.008	.078	.0044	.024
¹ 296	-	-	-	-	-	-	-	-	-
297	.001	.0042	-.005	.032	.0044	.004	.080	.0046	.019
298	.009	.0036	-.004	.037	.0039	.004	.078	.0051	.016
299	.003	.0039	-.007	.033	.0038	.000	.072	.0040	.010
¹ 300	-.089	-.0072	.027	-.076	-.0064	.030	-.043	-.0041	.046
	$\alpha = -4^\circ$			$\alpha = 0^\circ$			$\alpha = 8^\circ$		
¹ 301	-	-	-	-	-	-	-	-	-
	$\alpha = 0^\circ$			$\alpha = 4^\circ$			$\alpha = 12^\circ$		
302	0.009	0.0034	-.002	0.037	0.0041	0.003	0.081	0.0040	0.015
303	.010	.0033	-.001	.033	.0037	.004	.076	.0043	.013
304	.006	.0033	-.002	.034	.0037	.005	.071	.0055	.013
305	.007	.0033	-.003	.033	.0035	.004	.065	.0044	.018

¹ The values given represent the differences between the characteristics of each combination and those of the corresponding airfoil with full-span split flap.

TABLE V. - PRINCIPAL AERODYNAMIC CHARACTERISTICS OF WING-FUSELAGE COMBINATIONS

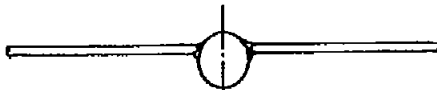

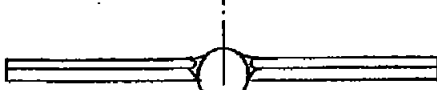
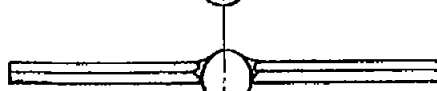

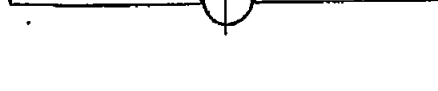

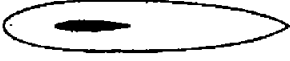


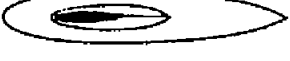



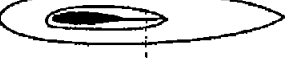

Diagrams representing combinations	Com- bina- tion	Remarks	Longi- tudinal posi- tion d/c	Verti- cal posi- tion k/c	Angle of wing setting γ (deg.)	Lift- curve slope (per degree) $\frac{1}{\alpha}$ $A=5.86$	Span effi- ciency factor ϵ	$C_{D_{min}}$	$C_{L_{opt}}$	Aerody- namic center position n_c	C_{M_0}	Lift coef- ficient at interference bubble ${}^1C_{L_{1b}}$	${}^2C_{L_{max}}$	
													Effec- tive R = 4.2 x 10 ⁶	Effec- tive R = 3.7 x 10 ⁶
Rectangular N.A.C.A. 23012 airfoil with round fuselage														
	-	Wing alone	-	-	-	0.078	0.85	0.0085	0.12	0.007	-0.007	^A 1.6	^a 1.61	^a 1.43
	-	Wing alone with full-span split flap deflected 60°	-	-	-	.074	-	0.17	-	-	0.21	-	^a 2.32	^a 2.24
	286	Tapered fillets; plaster finish.	0	.16	0	.062	0.85	.0117	.14	.016	-0.010	^A 1.5	^b 1.56	^b 1.48
	287	Tapered fillets; plaster finish; 60° split flap	0	.16	0	0.077	-	0.16	-	-	0.19	-	^a 2.10	^a 2.11
	289	L.E. fillets 1; plaster finish; 60° split flap	0	.16	0	0.079	-	0.16	-	-	0.19	-	^b 1.96	^b 2.01
	290	L.E. fillets 1; lacquer finish; 60° split flap	0	.16	0	-	-	-	-	-	-	-	^a 2.15	2.12
	291	L.E. fillets 1 lacquer finish; 60° split flap with trailing edge of fillets cut away	0	.16	0	-	-	-	-	-	-	-	^a 2.08	^a 2.10


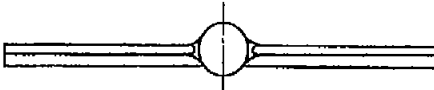





TABLE V. (Continued)

Diagrams representing combinations	Combination	Remarks	Longitudinal position d/c	Vertical position k/c	Angle of wing setting i_w (deg.)	Lift-curve slope (per degree) $A=6.86$	Span efficiency factor s	$C_{D_{min}}$	$C_{L_{opt}}$	Aerodynamic-center position X_c	C_{M_0}	Lift coefficient at interference burble $C_{L_{ib}}$	$C_{L_{max}}$	
													Effective $R = \frac{8.5}{10} \times$	Effective $R = \frac{5.7}{10} \times$
Rectangular N.A.C.A. 0012 airfoil with round fuselage														
	7	(From reference 1.) Plaster finish	0	0	0	0.080	0.85	0.0115	0.00	0.040	0.000	$R_{1.0}$	$b_{1.21}$	$b_{1.20}$
	292	Lacquer finish	0	0	0	.081	.85	.0115	.00	.038	-.005	$R_{1.1}$	$a_{1.20}$	$b_{1.19}$
	187	(From reference 1.) Tapered fillets; plaster finish	0	0	0	.081	.85	.0115	.00	.030	.000	$R_{1.0}$	$a_{1.23}$	$a_{1.22}$
	293	Tapered fillets; lacquer finish	0	0	0	.083	.85	.0114	.00	.030	-.002	$A_{1.3}$	$b_{1.33}$	$b_{1.30}$
	294	L.E. fillets 2; lacquer finish	0	0	0	.083	.85	.0119	.01	.048	-.004	$A_{1.5}$	$b_{1.30}$	$b_{1.30}$
	295	L.E. fillets 2a; lacquer finish	0	0	0	.083	.85	.0122	.01	.040	-.002	$A_{1.5}$	$a_{1.33}$	$b_{1.44}$
	296	L.E. fillets 2a; lacquer finish; 60° split flap	0	0	0	-	-	-	-	-	-	-	$a_{2.17}$	$a_{2.03}$
	297	L.E. fillets 2b; lacquer finish	0	0	0	.084	.85	.0122	.00	.043	-.005	$A_{1.5}$	$a_{1.33}$	$b_{1.47}$
	298	L.E. fillets 3, 0.6c span; lacquer finish	0	0	0	.084	.85	.0115	.00	.036	-.005	$A_{1.5}$	$a_{1.35}$	$a_{1.49}$

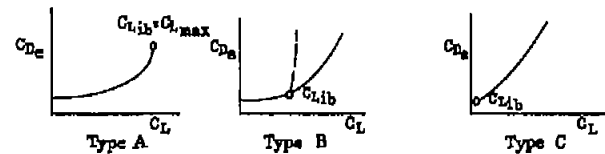
N.A.C.A. Technical Note No. 641

(Continued) on next page

TABLE V. (Continued)

Diagrams representing combinations	Com- bina- tion	Remarks	Longi- tudinal posi- tion d/o	Verti- cal posi- tion k/o	Angle of wing set- ting i_w (deg.)	Lift- curve slope (per degree) α $A=6.88$	Span effi- ciency factor ϵ	$C_{D_{e_{min}}}$	$C_{L_{opt}}$	Aerody- namic center posi- tion x_0	C_{M_0}	Lift coef- ficient at interfer- ence burbl $C_{L_{ib}}$	$C_{L_{max}}$	
													Effec- tive $R =$ $8.2 \times$ 10^6	Effec- tive $R =$ $3.7 \times$ 10^6
Rectangular N.A.C.A. 0012 airfoil with round fuselage														
	299	L.E. fillets 3a, 0.45c spans; lacquer finish	0	0	0	.088	⁴ .86	.0115	.00	.029	-.005	¹ 1.5	^a 1.84	^b 1.51
	300	L.E. fillets 3a, 0.45c spans; lacquer finish, with 80° split flap	0	0	0	⁷ .078	-	⁷ .17	-	-	⁷ -.18	-	^a 2.32	^b 2.14
Rectangular N.A.C.A. 4412 airfoil with round fuselage														
	301	Tapered fillets; lacquer finish; 50° split flap	0	0	0	⁷ .075	-	⁷ .15	-	-	⁷ -.24	-	^a 2.24	^b 2.20
Rectangular N.A.C.A. 0012 airfoil with round fuselage														
	302	L.E. fillets 5b, 0.3c spans; lacquer finish	0	0	0	.084	⁴ .85	.0114	.00	.028	-.003	¹ 1.5	^a 1.62	^b 1.42
	303	L.E. fillets 3c, 0.15c spans; lacquer finish	0	0	0	.085	⁴ .85	.0115	.00	.026	-.002	¹ 1.5	^a 1.55	^b 1.42
	304	L.E. fillets 3d, 0.075c spans; lacquer finish	0	0	0	.088	⁴ .85	.0114	.00	.029	-.002	¹ 1.4	^b 1.44	^b 1.26
	305	L.E. fillets 5c, 0.15c spans; lacquer finish, with fillet trailing edge cut away	0	0	0	.081	⁴ .85	.0113	.00	.020	-.003	¹ 1.4	^b 1.45	^b 1.29

¹Letters refer to types of drag curves associated with the interference burble as follows: ²Letters refer to condition at maximum lift as follows: ³Reasonably steady at $C_{L_{max}}$;



⁴small loss of lift beyond $C_{L_{max}}$; ⁵large loss of lift beyond $C_{L_{max}}$ and uncertain value of $C_{L_{max}}$.

⁶Poor agreement in high-speed range.

⁷Poor agreement over whole range.

⁸Poor agreement in high-lift range.

⁹Rapid increase in drag preceding definite breakdown.

⁷Value that is averaged over useful range.



Figure 1. - Combination 280, showing special leading-edge fillet 1.

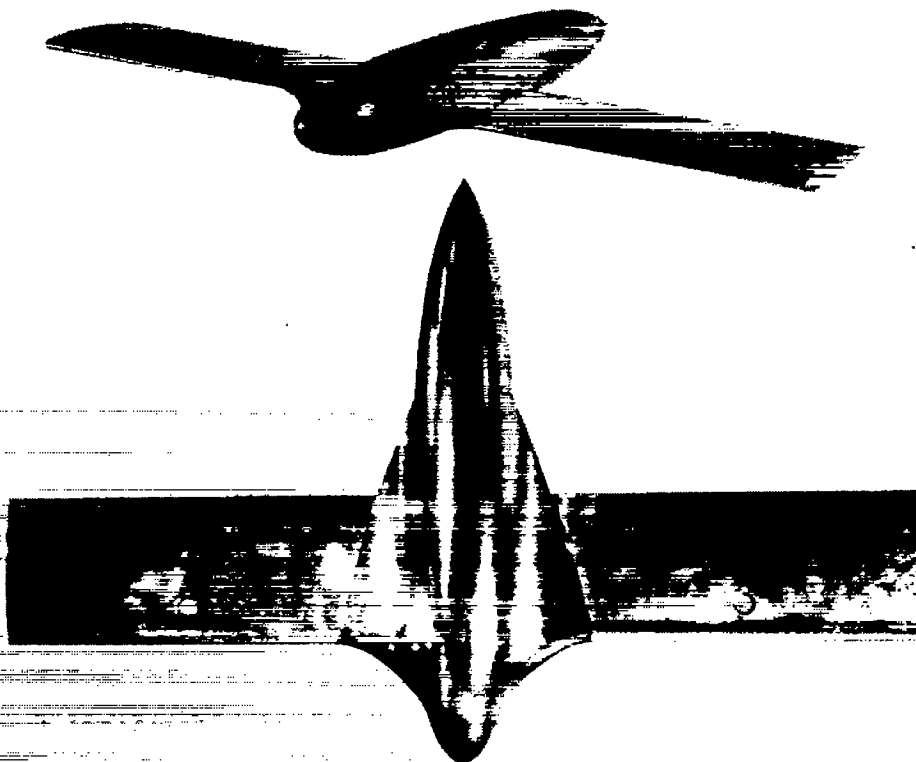


Figure 2. - Combination 294, showing leading-edge fillet 2.

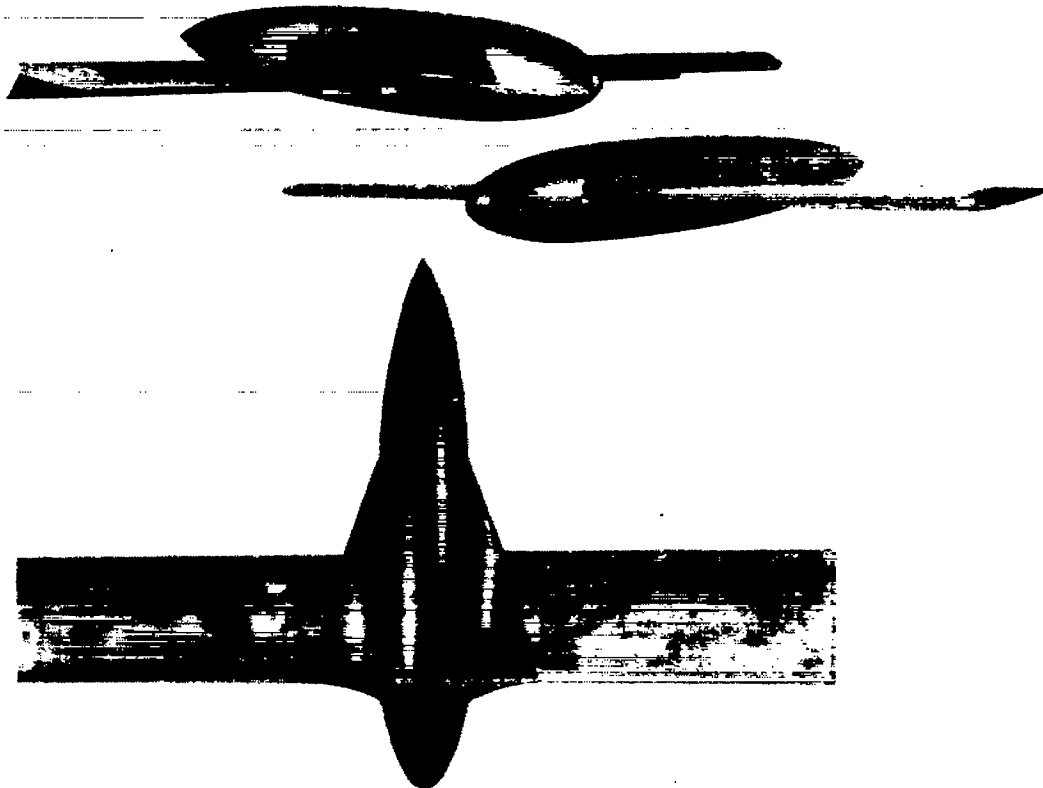


Figure 3. - Combinations 296 and 297 showing leading-edge fillets 2a (with flaps) and 2b.

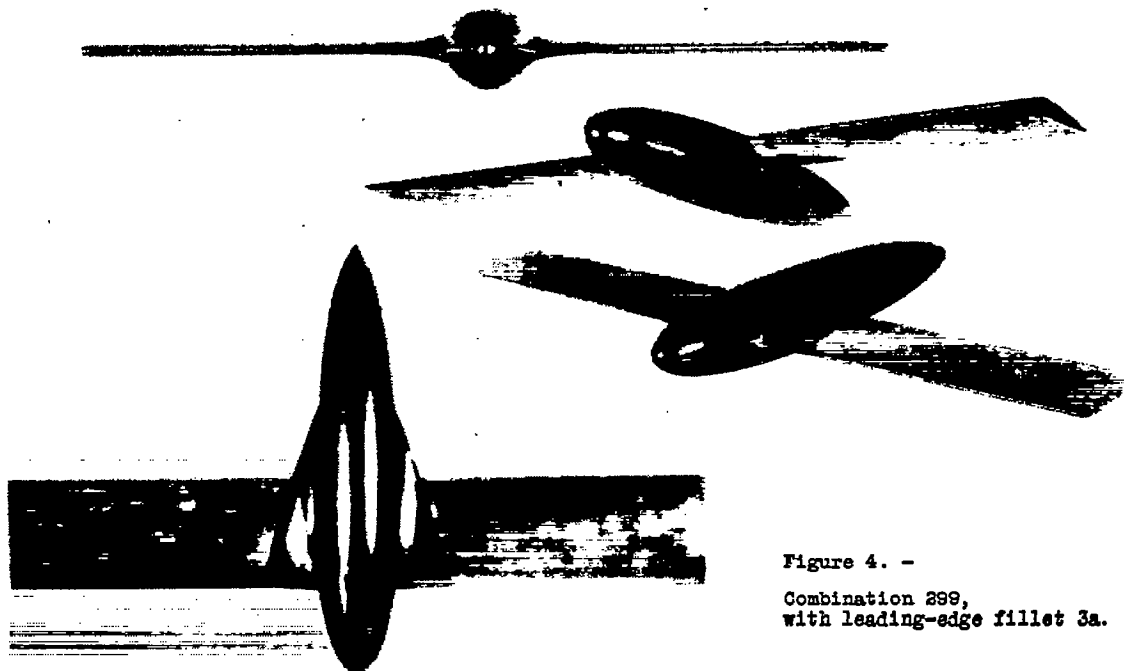


Figure 4. -
Combination 299,
with leading-edge fillet 3a.

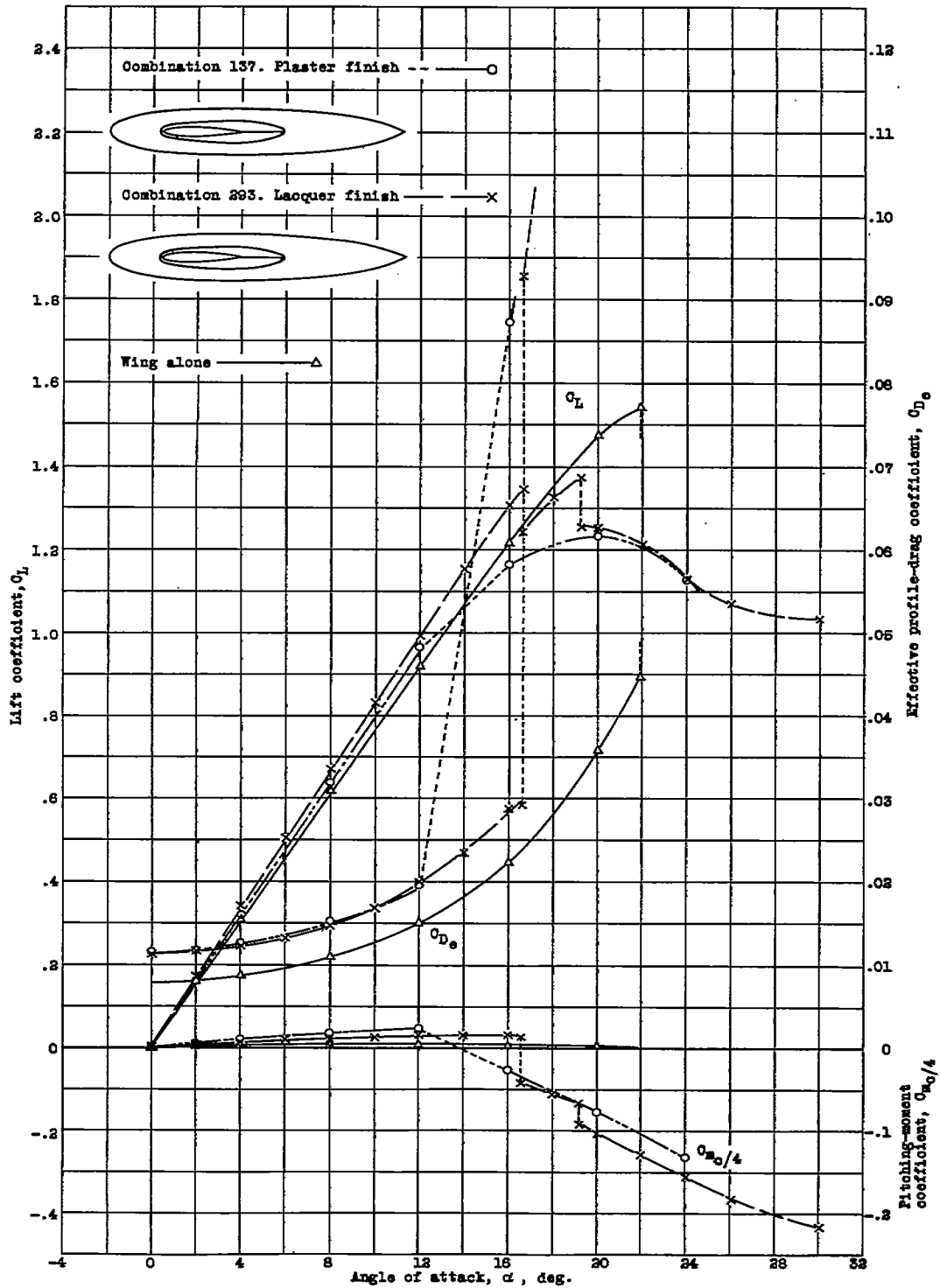


Figure 5. - Effect of surface finish at junctures of a critical wing-fuselage combination. Rectangular N.A.C.A. 0012 airfoil and round fuselage with tapered fillets. Midwing position.

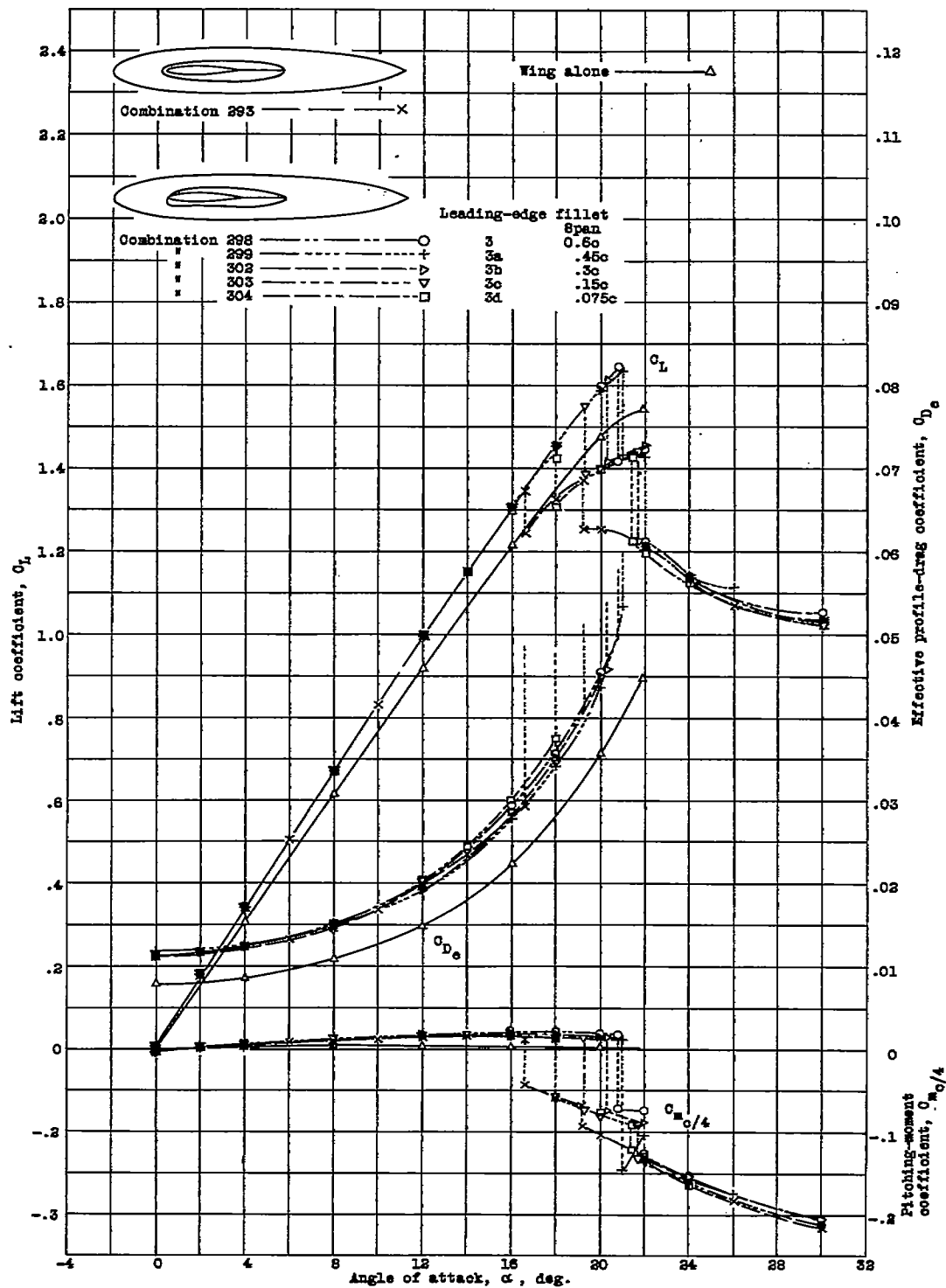


Figure 6. - Effect of special leading-edge fillets on the interference burble. Rectangular N.A.C.A. 0012 airfoil and round fuselage. Midwing position.

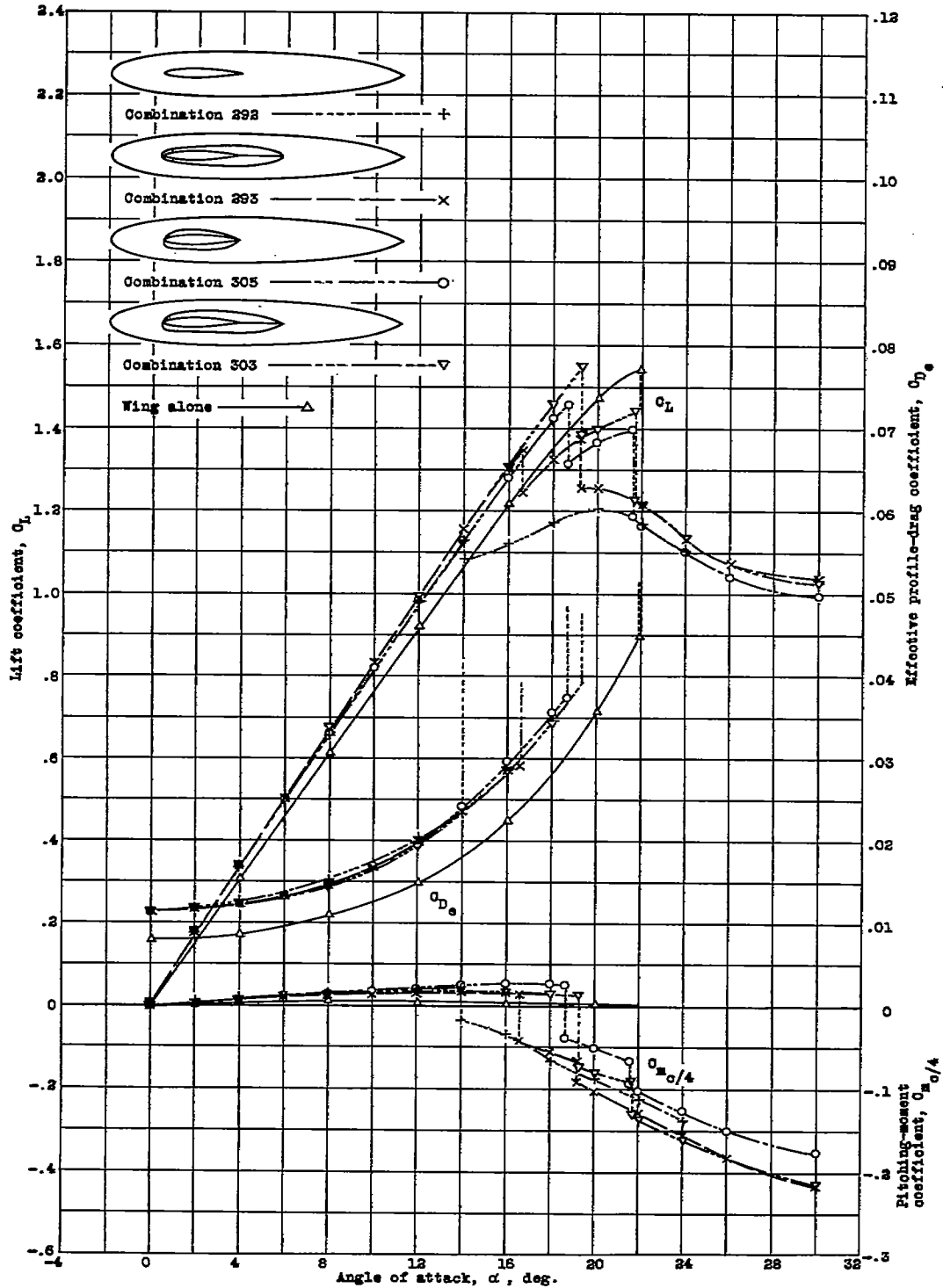


Figure 7. - Characteristics for various fillet shapes. Rectangular N.A.C.A. 0012 airfoil and round fuselage. Midwing position.